

Ion Homeostasis in Spatially Polarized Excitable Cells: An Approach to Maximize Endogenous Electric Fields

Maxim Piatine

Supervisor: Bela Joos

April 29, 2024

Abstract

Understanding the dynamics of ion flux and polarization in spatially polarized excitable cells is crucial for fundamental physiological processes such as wound healing, muscle contraction, and nerve impulse transmission. This study investigates a charge difference model as a two-compartmentalized cell connected by a gap junction. Through theoretical analyses and simulations, we explore the result of symmetry breaking by manipulating ion permeability ratios and elongating the cell on endogenous electric fields. Our findings reveal that symmetry breaking can significantly enhance endogenous electric field strength while staying within realistic constraints. Our results provide valuable insights into cellular polarization mechanisms and offer implications for future research in cell physiology.

Contents

1	Introduction	5
2	Background and Context	6
2.1	Background	6
2.2	Achieving Ion Homeostasis	7
2.3	Zero Dimension Steady State	9
2.4	Anterior Posterior Charge Difference Model	10
2.5	Symmetry Breaking	12
3	Scientific Methods	14
3.1	Definitions	14
3.2	Cytoplasmic voltage	15
3.3	Drift current density	15
3.4	Transmembrane current	17
3.4.1	Leak current	18
3.4.2	ATPase pump current and consumption	18
3.4.3	Co-transporter	19
3.5	Nernst potentials	19
3.6	Charge difference and resting membrane potential	20
3.7	Number of intracellular ions	20
3.8	Cell Volume	20
3.9	Cytoplasmic Donnan effectors	21
3.10	Steady state	22
3.11	Maximizing endogenous electric field	23
4	Results	24
4.1	Parameters	24
4.2	Data Analysis	25
4.2.1	Anterior double P_{Na} and half P_K	25
4.2.2	Elongation of gap junction	26
4.2.3	Anterior Posterior symmetry breaking	30
4.3	Discussion	32

1 Introduction

Evolutionary cells have found a way to sustain themselves through various methods, one of which is regulating ion flux in the cell. Allowing for the passage of potassium (K^+), sodium (Na), and chloride (Cl^-) ions to move across the cell membrane and navigate against their concentration gradient. Ions diffusing through regions of lower concentration is also known as active transport, maintaining cellular equilibrium.

Potassium ions concentrate intracellularly, diffusing outside the cell walls through their respective gates or leak channels. Sodium and chloride concentrate on the outside of the cell, and they manage to find themselves inside the walls of the membrane through different gates spread across the membrane, such as the voltage-gated or leak channels.

The movement of ions across the cell membrane plays a crucial role in cell polarization. As ions move in and out of the cell, they create electrical potential differences across the membrane, leading to a resting membrane potential. Polarization is pivotal in understanding muscle contraction, wound healing, and nerve impulse transmission, as it creates endogenous electric fields.

Furthermore, polarization enables endogenous electric fields within the cell, as demonstrated in Ziyi Liu's thesis paper, "Developing Tools towards Ion Homeostasis in Spatially Polarized Excitable Cells." Liu introduces a one-dimensional charge difference model, the posterior anterior-charge difference model PA-CD, that analyzes a two-compartmentalized cell separated by a gap-junction and the parameters that improve the endogenous electric field. [1]

This paper aims to optimize the endogenous electric field within the constraints observed or simulated in biophysics studies. Using these parameters in Liu's thesis paper, we strive to understand the function of endogenous electric fields.

2 Background and Context

2.1 Background

The skin can generate an electric field in response to tissue damage in wound healing and cell migration. When disrupted, the epithelial layer creates an endogenous electric field within the injured tissue, which migrates local cells to reseal the damaged epithelial layer. Cells such as the keratinocytes in humans can detect electric fields and respond with directed migration. [2]

Interestingly, endogenous electric fields around the wound act like batteries, having an exciting polarity to navigate the cells and ions toward the area of attraction. Additionally, the polarity fluctuates after certain stages of the healing process, becoming negatively charged. [3]

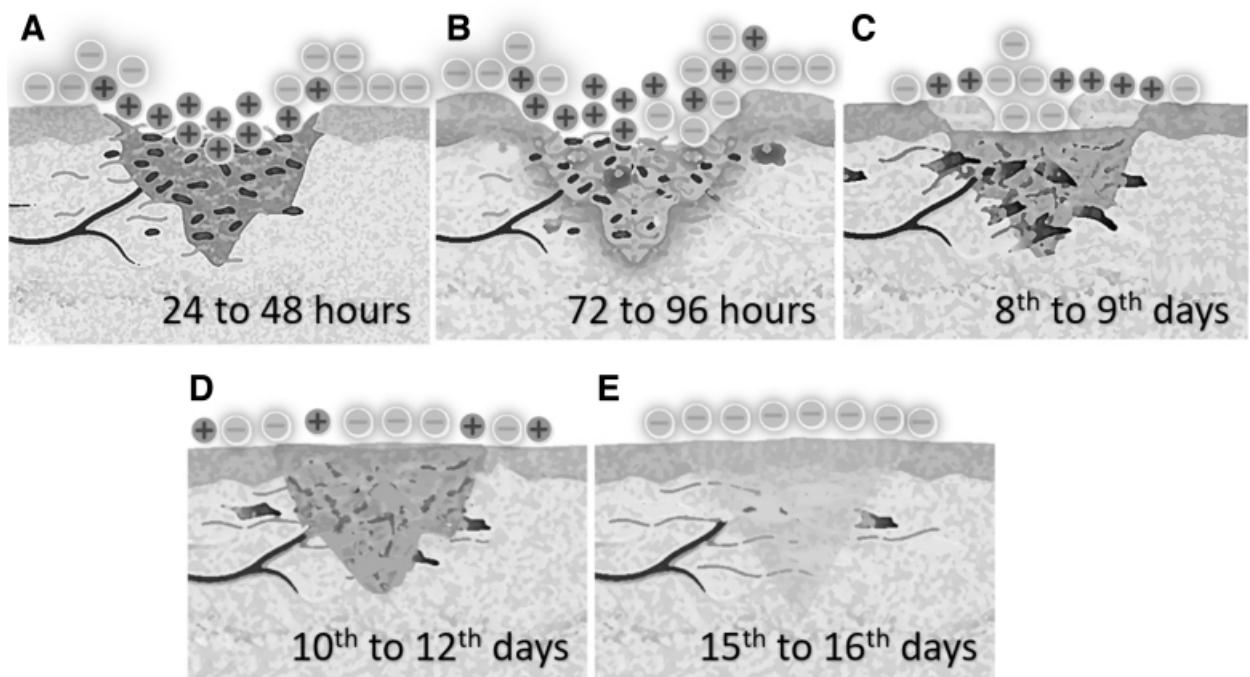


Figure 2.1 **Fluctuation of electric field after injury**. Figure taken from Paulo Luiz Farber, "Electric Factors in Wound Healing", depicting the movement of charges as a time progression in wound healing.

2.2 Achieving Ion Homeostasis

Ion homeostasis is a set point at which a cell maintains an intracellular ion concentration, cell volume, and transmembrane potential set by the steady state of the cell and regulates the movement of ions and water across the cell membrane and a number of valences for impermeant ions through passive and active functions. [6]

Cells evolved to develop different functions to maintain this balance through membrane channels that leak, pump, and transport water and these different ions in and out of the cell. These functions are known as the Pump-leak Donnan process (P-L/D). The main pump-leak channels correspond to sodium and potassium. The Donnan channels regulate the movement of ions based on charge differential.

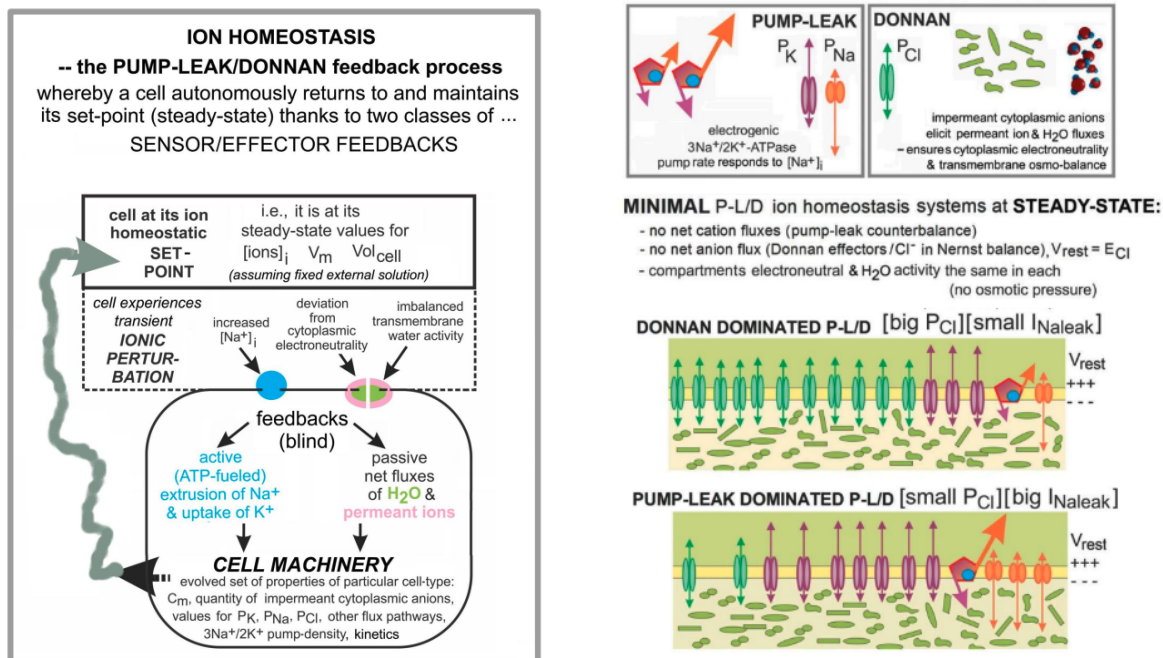


Figure 2.1 P-L/D ion homeostasis

One functionality of the cell membrane channels includes the permeability leaks for ions. These leaks are passive ways for ions to move against their gradient levels, allowing them to enter and leave the cell through these channels to their respective ion leak channels. Due to the high concentration of ions on the outside of the cell, chloride and sodium migrate towards the inside. On the contrary, potassium is heavily concentrated intracellularly, thus leaking towards the outside. As ions move through the cell membrane, due to the Nernst-Planck equation, they cause the resting membrane voltage potential to change from -70.22 mV. Steady-state permeable leaks, found in Table 2.1, provide a

volume of ions per second, resulting in a different membrane potential if there are no functions that moderate this influx.

$$V_{Nernst} = V_{in} - V_{out} = -\frac{k_b T}{q} \ln \frac{c_{in}}{c_{out}}$$

Luckily, ATPase autonomously pumps the excess outside and the lack inside to regulate intracellular and extracellular concentration levels and bring the cell back to its resting potential. Na⁺/K⁺ ATPase pumps 3Na⁺ out of the cell and 2K⁺ into the cell for every single ATP consumed. The pumps are a byproduct of evolution; cells must regulate the ions intracellularly. Through sensory feedback, the ATP responds to the excess sodium intracellularly to actively and "blindly" pump them out. The process repeats itself, maintaining resting potential and regulating cellular volume.

Donnan effects influence the distribution of permeable ions to neutralize the impermeable cations, like proteins, through the semi-permeable membrane against their charge and concentration gradients. Impermeable ions create an osmotic pressure gradient caused by the difference in solute concentration, where water is needed to maintain the osmotic balance through permeable membranes. Therefore, establishing and maintaining electrochemical gradients across cellular membranes.

Cells achieve cellular homeostasis either through Pump-Leak or Donnan-dominant mechanisms. Neuron cells are mostly Pump-Leak-dominant and skeletal muscles are Donnan-dominant.[1] The paper focuses on pump-leak-dominated cells, which, have few permeable chloride channels.

$$P_K \gg P_{Na} > P_{Cl}$$

Consequently, the permeability ratio between sodium and potassium leak permeability characterizes the resting membrane potential. From Table 2.1, the ratio causes the resting membrane voltage potential to be -70.22 mV. Notably, the ratio between P_{Na+} and P_{K+} either hyperpolarizes or depolarizes the membrane potential. A sufficiently large depolarization in excitable cells in a short period causes action potential. From Morris et al., "The Donnan-Dominated Resting State of Skeletal Muscle Fibers Contributes to Resilience and Longevity in Dystrophic Fibers," according to Figure 4D, as the ratios P_{Na+} and P_{K+} increase, so does the resting membrane potential. [6]

2.3 Zero Dimension Steady State

Cells achieve ion homeostasis by stabilizing different ions intracellularly, the cell's volume, and the membrane potential with different "pump leak mechanisms." [1] These set points were carefully studied and analyzed and are essential parameters to include in the simulation for a singular cell compartment.

Table 2.1 Zero dimension parameters in steady state

Definition	Parameter	Unit	Value
Cell Volume	Vol_{cell}	μm^3	2000
Membrane Potential	V_{rest}	mV	-70.22
Extracellular/Intracellular Sodium Concentration	$[Na^+]$	mM	152/7.84
Extracellular/Intracellular Potassium Concentration	$[K^+]$	mM	3/147.16
Extracellular/Intracellular Chloride Concentration	$[Cl^-]$	mM	135/9.74
Extracellular/Intracellular Anions Concentration	$[An^-]$	mM	20/145.26
Leak Sodium Permeability	P_{Na}	$\mu m^3/s$	1.51
Leak Potassium Permeability	P_K	$\mu m^3/s$	20
Leak Chloride Permeability	P_{Cl}	$\mu m^3/s$	2.5

Based on the "Biophysical Model for Cytotoxic Cell Swelling" paper by Dijkstra, Table 1 presents parameters of intracellular conditions for neuron cells in a steady state. [4] In the case of the PA-CD model, both anterior and posterior cells live in the same conditions in a steady state and are symmetric. This paper aims to observe the breaking of symmetry, which includes manipulating steady-state parameters to influence ion fluctuations through the cell membrane, causing drift and diffusion current that leads to an endogenous electric field.

By analyzing permeability channels for different ions, we can see that there is a change in membrane potential whenever there is an increase or decrease in ion movement intracellularly or extracellularly through these channels. In zero dimensions, to achieve a membrane resting potential of -70.22 mV, the permeability would need to be precisely in the ratio of $P_{Na} : P_K$, which is 0.0755, considering that chloride permeable ions do not affect the membrane potential due to the lack of concentration.

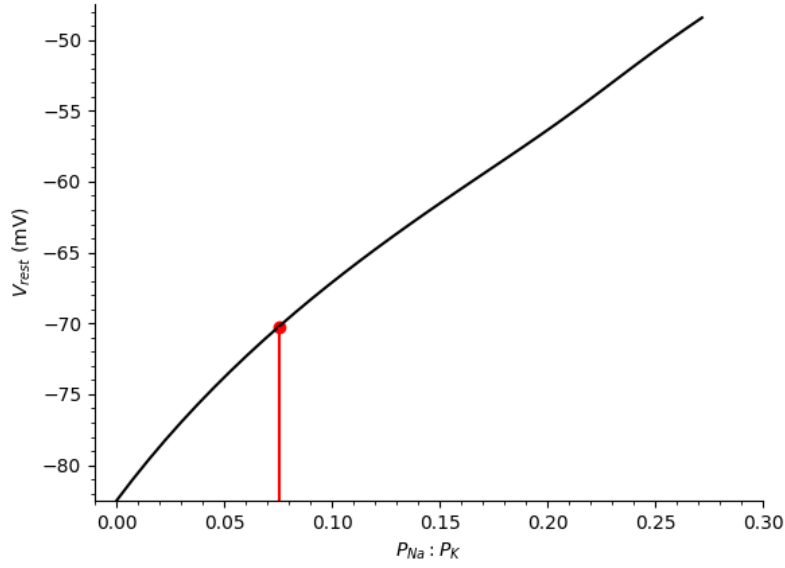
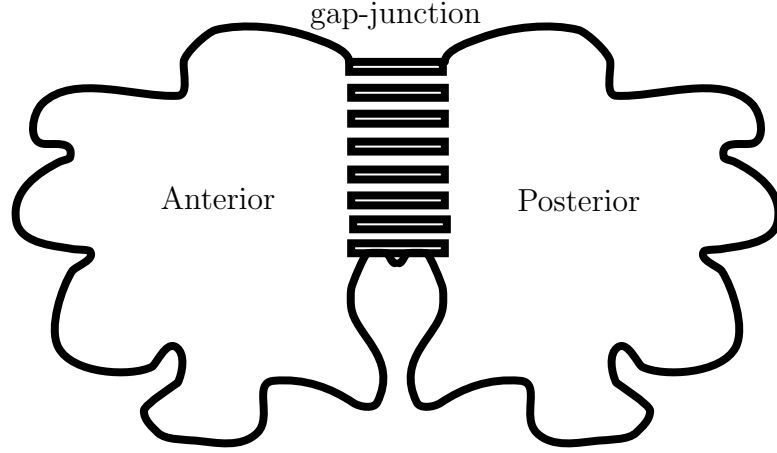


Figure 2.2 **Permeability ratio in zero dimension.** Graph depicting the membrane potential increase as the leak permeable ratios change. The red intersection is the resting membrane potential when the ratio between sodium and potassium permeability remains at $1.51 \mu m^3/s$ and $20 \mu m^3/s$, respectively, causing the intersection to be at 0.0755 and -70.22 mV.

Figure 2.2 suggests that we can adjust the ratios of permeabilities to enhance the resting membrane potential. With a ratio of 0.0755, the resting membrane potential's midpoint is -70.22 mV. However, increasing the ratio to 0.3 means the membrane resting potential would cap at -50 mV.

2.4 Anterior Posterior Charge Difference Model

The charge difference model starts by determining the ion flux through the cell's membrane to identify its steady state. The steady-state information includes the cell's volume, the concentration of ions intracellularly, and the resting membrane potential. The charge difference model uses the cellular components of a cell to calculate the steady state using the Nernst-Planckian diffusion and drift. Using ion homeostasis and the charge difference model, we can calculate the steady state values of a cell.



The PA-CD model acts like a singular cell in conditions both the posterior and anterior cells experience. The previous section, "Zero Dimension Steady State," referenced that having a ratio of sodium and potassium ions influences the membrane's resting potential. Utilizing this idea, having the same anterior and posterior leak permeabilities will make the PA-CD model act like a singular cell. The objective of the PA-CD model in this context is to maximize the cytoplasmic voltage through the drift and diffusion of ions in the cytoplasm. Meaning, through the different ratios of the anterior and posterior leak permeabilities, determine the steady state endogenous electric field from the ion fluxes from one cell to the other.

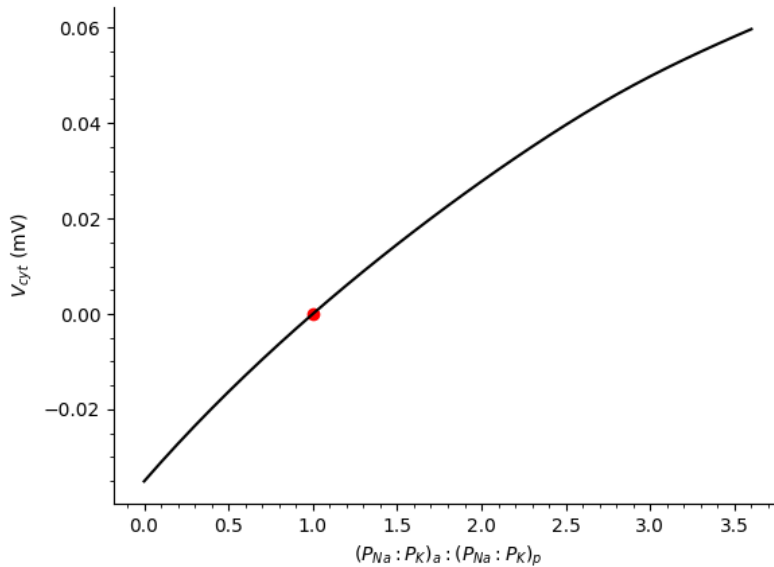


Figure 2.3 Permeability ratio and cytoplasmic voltage. The balance of permeabilities between the anterior and posterior results in no cytoplasmic voltage, as the red dot shows. By changing the ratio from 1 to 1, the achievement of cytoplasmic voltage increases or decreases depending on which cell increases the permeability ratio.

$$P_{Na+,p} : P_{K+,p} = P_{Na+,a} : P_{K+,a} \rightarrow E \approx 0$$

The ratio formula above explains that the similarity between anterior and posterior permeability leads to an approximately zero endogenous electric field, assuming chloride permeability has no impact on it.

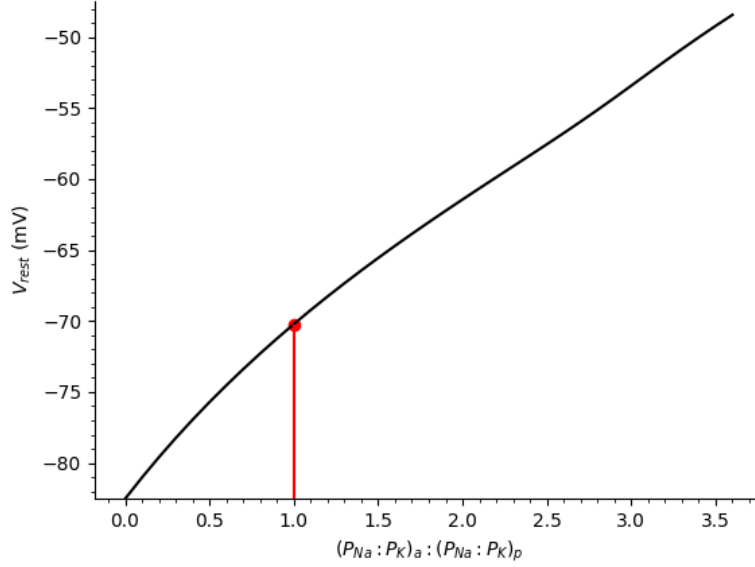


Figure 2.4 **Permeability ratio and resting membrane potential.** The increasing change in permeability ratio increases the membrane resting potential for both anterior and posterior.

Similar to the zero-dimensional subsection, as permeability increases, so does membrane potential. In the case of Figure 2.4, the anterior and posterior membrane potential overlap as they are similar when the permeability leak ratio increases.

2.5 Symmetry Breaking

In the last section, parameters were covered that are considered set points for the cell to be in ion homeostasis. In the context of the PA-CD model, it would result in both cells being in ion homeostasis, which allows two-compartment cells to still play a role in migrating and wound healing, thus being a consequence of some endogenous electric field to be present. However, these conditions significantly limit the induced electric field; this paper seeks to maximize these fields by breaking the symmetry through various combinations by isolating the anterior and posterior cells.

In symmetry breaking, the posterior and anterior cells are taken as two compartments going through different stages of polarization. By isolating one compartment, one compartment goes through the regulatory processes of ion homeostasis, and the other influences the permeability rate of ions to create more membrane potential; this means that while one cell reaches regulatory steady state, the other moves the set points of steady state, which results in concentration levels, and membrane potential to change. Therefore, it creates ion movement intracellularly, which causes diffusive and drift currents. Figure 2.3 provides the idea of separating the anterior and posterior permeabilities. As the ratio of permeabilities increases in the anterior cell and decreases in the posterior cell, there is an increase in cytoplasmic electric potential.

Moreover, separating the two compartments with a more prolonged gap junction causes more endogenous electric fields due to the resistance factor. Ohm's law dictates the voltage potential through current and resistance, causing the electric field to increase due to voltage potential.

$$\begin{aligned} V &= IR \\ E &= \frac{V}{d} = \frac{\Delta V_{cyt}}{\Delta x_{ref}} \end{aligned} \tag{2.1}$$

Formula 2.1 derives the endogenous electric E field using Ohm's law, where V is the cytoplasmic voltage potential, I is the cytoplasmic current, R is the resistance in gap-junction, and Δx_{ref} is the reference size of a generic cell.

To summarize, breaking the symmetry of the two-compartment cell increases the endogenous electric field. Two methods that achieve large electric fields are to elongate the cell with the gap junction to create more resistance and manipulate the permeability ratio to be lower or higher for one cell while the other experiences the opposite polarization. That way, the different cell will compensate wherever there is a lack of ions in the other cell.

3 Scientific Methods

3.1 Definitions

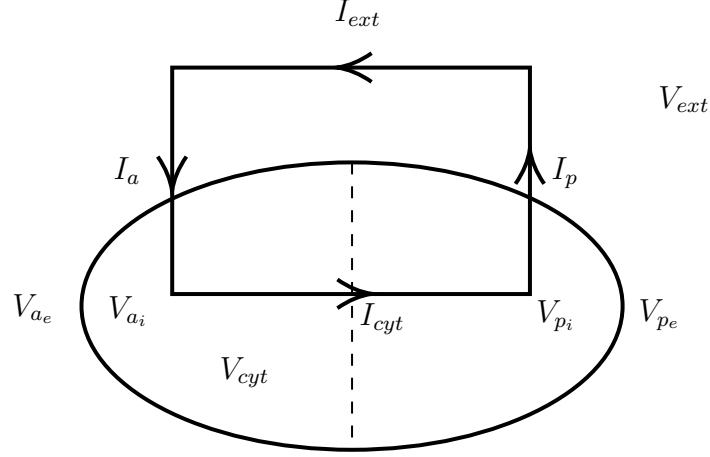


Figure 3.1 **PA-CD Model**. A two-compartment cell separated by a gap junction. V_{ae} and V_{pe} are exterior membrane voltages of the anterior and posterior compartments. V_{ai} and V_{pi} are interior membrane voltages of the anterior and posterior compartments. I_a and I_p are transmembrane currents equal in steady state. I_{ext} is the external current, and I_{cyt} is the cytoplasmic current coming from the diffusion and drift of the currents. V_{ext} is the voltage outside of the cell, and V_{cyt} is the voltage inside.

Before going into the theoretical calculations, let us define some variables:

$$V_p = V_{pi} - V_{pe} \quad (3.1)$$

Where V_p is the voltage potential difference between the posterior membrane wall's interior (i) and exterior (e). Similarly, for the anterior potential difference:

$$V_a = V_{ai} - V_{ae} \quad (3.2)$$

Difference potential of cytoplasm is the difference of interior voltages. Contrarily, the exterior potential difference is the difference between exterior potentials:

$$\Delta V_{cyt} = V_{ai} - V_{pi} \quad (3.3)$$

$$\Delta V_{ext} = V_{a_{ext}} - V_{p_{ext}} \quad (3.4)$$

3.2 Cytoplasmic voltage

From the background, there is an understanding that a large amount of ions are moving around in and out of the cell, constantly drifting and diffusing. We assume that the exterior concentration of the cell is homogeneous; therefore, we can suppose that the exterior current I_{ext} is ohmic in nature and has no diffusion, only drift.

$$\begin{aligned} I_{ext} &= \frac{\Delta V_{ext}}{R_{ext}} \\ \Delta V_{ext} &= I_{ext} R_{ext} \end{aligned} \tag{3.5}$$

Using Kirchhoff's law, we can set up our equation as:

$$\begin{aligned} 0 &= -V_a + \Delta V_{cyt} + V_p + \Delta V_{ext} \\ \Delta V_{cyt} &= V_a - V_p - V_{ext} = V_a - V_p - I_{ext} R_{ext} \end{aligned} \tag{3.6}$$

Where ΔV_{cyt} is the cytoplasmic voltage potential, which will be used to calculate the endogenous electric field in equation (2.1).

3.3 Drift current density

The Nernst-Planck equation, used for the movement of ions, determines ions' diffusion and drift currents in the anterior and posterior membranes.

$$J = \Delta c v_d = c_o \frac{F}{\gamma} \tag{3.7}$$

v_d is the drift velocity characterized as the force F of friction constant γ . Leading to replacing the γ constant with Einstein's relation $D\gamma = k_b T$, and the force by the force of electric field $F = zeE$, where E is the electric field strength that can be represented by $E = \frac{\Delta V_{cyt}}{\Delta x_{ref}}$ shown in equation (2.1). Where the ΔV_{cyt} shown in equation (3.6) is the difference between anterior-posterior and external voltages, and Δx_{ref} is the reference size of the cell.

$$J = \Delta c \times \frac{D}{k_b T} \times ze \times \frac{\Delta V_{cyt}}{\Delta x_{ref}} \tag{3.8}$$

Where current can be represented using the Fick's law relation across a cross-sectional area:

$$\begin{aligned}
I &= J \times ze \times A \\
&= \Delta c \times \frac{D}{k_b T} \times ze \times \frac{\Delta V_{cyt}}{\Delta x_{ref}} \times ze \times A \\
&= \left(\Delta c \times \frac{D}{k_b T} \times (ze)^2 \times \frac{A}{\Delta x_{ref}} \right) \times \Delta V_{cyt} \\
&= \frac{1}{R_{cyt}} \times \Delta V_{cyt}
\end{aligned} \tag{3.9}$$

Where z represents the ions' valence, Δc is the concentration difference of ions between anterior and posterior cells, D is the diffusion coefficient of an ion, e is the charge constant, k_b is the Boltzmann constant, T temperature, and A cross-sectional area. More details can be found in Table 3.1, documenting every constant in these equations. Remember that every ion moving within the cell will have different valence, concentration differences, and diffusion coefficients.

$$R_{cyt} \propto \Delta x \tag{3.10}$$

Making the resistance R_{cyt} proportional to the distance Δx , which is the distance from the center of both cells, which includes the gap-junction:

$$R_{cyt} = \frac{k_b T \Delta x}{DA(ze)^2 c_o} \tag{3.11}$$

$$= \frac{k_b T \Delta x_{ref}}{DA(ze)^2 \Delta x} \times \frac{\Delta x}{\Delta x_{ref}}$$

F is the Faraday constant that replaces $e \times N_A$, R is the gas constant that replaces the Boltzmann constant with $k_b N_A$, where N_A is the Avogadro constant. The ohmic resistance from equation (3.9) has the form:

$$R_{cyt} = \frac{RT}{ze^2 N_A} \times \frac{\Delta x_{ref}}{DA \Delta c} \times \frac{\Delta x}{\Delta x_{ref}} \tag{3.12}$$

From equation (3.9), the derivation proceeds to separate the drift and diffusion current for solutes:

$$I_{diff} = \frac{-zFD\Delta c}{\Delta x_{ref}} \quad (3.13)$$

$$I_{drift} = \frac{-zF^2DA\Delta c\Delta V_{cyt}}{RT\Delta x_{ref}} \quad (3.14)$$

Thus, the diffusive and drift currents in equations 3.12 and 3.13, to have positive current from diffusion and drift $\frac{\Delta c}{\Delta x}$ and $\frac{\Delta V}{\Delta x}$ need to be smaller than zero.

Using the ohmic relation, we determined the correlation between resistance and gap junction and between the drift and diffusive currents inside the cell. Therefore, for each ion and anion in the cell, the cytoplasmic current looks like:

$$I_{cyt} = \sum_X I_{drift}^X + I_{diff}^X \quad \text{where } X \in \{Na^+, K^+, Cl^-, A^-\} \quad (3.15)$$

3.4 Transmembrane current

Transmembrane current I_{trans} is associated with the movement of ions through the membrane. Previously mentioned, in ion homeostasis, the movement of ions through passive and active channels cause a membrane potential. Passive and active channels such as leak channels and pumps are at the forefront at the cell wall maneuvering ions in and out of the cell creating from it a transmembrane current that is then calculated to obtain the transmembrane potential.

We mentioned that there are three main ions that contribute to membrane potential, those ions are the sodium Na^+ , potassium K^+ , and chloride Cl^- . Potassium is located intracellularly and moves against its concentrated gradient outside of the cell through leak channel I_L , and vice versa for sodium and chloride. Pump channels are there to maintain the level of concentration intracellularly due to their sensory feedback and pump 3 sodium out with an uptake of 2 potassium ions in creating the pump current I_{pump} . Along with the pump current there are protein co-transporters represented by J that come along with Faraday's constant in the equations below.

$$I_{trans}^{Na} = I_L^{Na} + 3I_{pump} - FJ_{NaKCl} \quad (3.16)$$

$$I_{trans}^K = I_L^K + I_{pump} + FJ_{KCl} - FJ_{NaKCl} \quad (3.17)$$

$$I_{trans}^{Cl} = I_L^{Cl} + FJ_{KCl} - FJ_{NaKCl} \quad (3.18)$$

$$I_{\text{tot trans}} = I_{trans}^{Na} + I_{trans}^K + I_{trans}^{Cl} \quad (3.19)$$

The following sections will mention the leak currents, pump currents, and the co-transporter mentioned in equations (3.16)-(3.18). Notably, the collection of all the ions moving across the anterior or posterior membrane will result in the membrane current $I_{\text{tot trans}}$ for that particular cell.

3.4.1 Leak current

Currents resulting from permeable passive channels are modelled using the GHK formula. [6]

$$I_{GHK} = I_{Leak}^X = P_{Leak}^X \frac{z_X^2 F^2 V}{RT} \left(\frac{[X]_i - [X]_e \exp - \frac{z_X FV}{RT}}{1 - \exp - \frac{z_X FV}{RT}} \right) \quad (3.20)$$

Where P_{Leak}^X is the anterior or posterior leak permeability value for ion X , where $X \in \{Na^+, K^+, Cl^-\}$. z_X is the valence of ion X . $[X]_i - [X]_e$ concentration difference intracellular and extracellular.

3.4.2 ATPase pump current and consumption

The electrogenic $3Na^+/2K^+$ ATPase follows:

$$\frac{I_{pump}}{Q_{pump}} = \frac{0.62}{1 + \left(\frac{6.7mM}{[Na^+]_i} \right)^3} + \frac{0.38}{1 + \left(\frac{67.6mM}{[Na^+]} \right)^3} \quad (3.21)$$

$$\begin{aligned} I_{pump} &= I_{pump}^{Na^+} + I_{pump}^{K^+} \\ &= \frac{1}{3} I_{pump}^{Na^+} = -\frac{1}{2} I_{pump}^{K^+} \end{aligned} \quad (3.22)$$

Q_{pump} is the maximum pump strength, and the I_{pump} is a hyperpolarizing sodium outflow.[6] The 0.62 and 0.38 constants in the numerator represent the receptor protein concentration proportions, with sodium binding sites $6.7mM$ and $67.6mM$. [1]

While the cell leaks sodium into the cell and potassium out, ion homeostasis takes care of that by letting the pump remove three sodium ions with the uptake of two potassium; for every three sodium and two potassium, the pump uses energy. The ATP consumption is measured as follows:

$$ATP/s = \frac{I_{pump}}{F} \quad (3.23)$$

3.4.3 Co-transporter

The Na-K-Cl and K/Cl co-transporters are membrane transport proteins that move ions into and out of the cell, respectively, and use the ions accordingly to maintain electroneutrality. With every positive ion comes a chloride.

The Na-K-Cl co-transporter is a protein with the secondary function of transporting sodium, potassium, and chloride into the cell. There are two isoforms of the membrane transport protein NKCC. Our model will focus on the NKCC1, which is found in almost all cell types. Similarly to the Nernst potential equation in subsection 3.5, the equation follows:

$$J_{NKCC} = U_{NKCC} \frac{RT}{F} \ln \left(\frac{[Na^+]_i [K^+]_i ([Cl^-]_i)^2}{[Na^+]_e [K^+]_e ([Cl^-]_e)^2} \right) \quad (3.24)$$

The K-Cl co-transporter is a membrane transport protein that moves the potassium and chloride ions out of the cell. Similarly to equation (3.24), the co-transporter has a Nernst-like equation of the form:

$$J_{KCl} = U_{KCl} \frac{RT}{F} \ln \left(\frac{[K^+]_i [Cl^-]_i}{[K^+]_e [Cl^-]_e} \right) \quad (3.25)$$

U_{KCl} and U_{NKCC} are the maximum flux capacity of the K/Cl co-transporter for their respective equation. [1]

3.5 Nernst potentials

Briefly mentioned in the background, it was mentioned that the movement of ions and the concentration differences between the inside and outside of the cell cause an electrical potential that can be measured via the Nernst potential formula:

$$E_X = V_{in} - V_{out} = \frac{RT}{z_X F} \log \frac{[X]_{in}}{[X]_{out}} \quad (3.26)$$

3.6 Charge difference and resting membrane potential

The charge difference model uses the known idea of ion movement to determine the potential across the membrane. The membrane potential function sets the standard resting membrane potential. As ions move, there will always be a equilibrium of influx and outflux of ions, creating a balance which results in resting membrane potential. At a steady state, the membrane potential depends on sodium and potassium leak current, which balances out with the strength of the pump, diffusion, and drift, which results in the resting membrane potential.

$$\begin{aligned} V_a = V_p &= \frac{F}{C_m} (N_i^{Na+} + N_i^{K+} - N_i^{Cl-} - N_i^{A-}) \\ &= \frac{F}{C_m} (dN^{Na+} + dN^{K+} - dN^{Cl-} - dN^{A-}) \end{aligned} \quad (3.27)$$

Where $dN^X = N_i^X - N_{i,0}^X$ is the difference in the number of ions between present N_i^X and reference value $N_{i,0}^X$, which produces a neutral membrane potential.[1] Membrane voltages are categorized by the potential voltage at both the anterior/posterior cell.

3.7 Number of intracellular ions

The charge difference model computes the change in intracellular ions [1], [6]:

$$\frac{dN^{Na+}}{dt} = -\frac{1}{F} (I_L^{Na} + I_{pump}) - J_{NKCC} \quad (3.28)$$

$$\frac{dN^{K+}}{dt} = -\frac{1}{F} (I_L^K + I_{pump}) J_{KCl} - J_{NKCC} \quad (3.29)$$

$$\frac{dN^{Cl-}}{dt} = -\frac{1}{F} (I_L^{Cl}) - J_{KCl} - J_{NKCC} \quad (3.30)$$

3.8 Cell Volume

Due to the flow of water J_{H_2O} , the volume of the cell changes. The rate at which the volume changes $\frac{dVol_{cell}}{dt}$ over time relies on the osmotic gradient across the membrane.

$$J_{H_2O} = \frac{dVol_{cell}}{dt} = P_{H_2O} \Delta Osm \quad (3.31)$$

$$\text{where } \Delta Osm = RT ([Sol]_i - [Sol]_e) \quad (3.32)$$

The P_{H_2O} is the effective membrane water permeability, and ΔOsm is the osmolyte gradient where $[Sol]_i$ and $[Sol]_e$ are the total concentrations intracellularly and extracellularly. Notable, the volume change rate is determined by the osmotic ion fluxes, not

the water flux. Compared to the ion fluxes, the osmotic gradient equilibration is nearly instantaneous. [1]

3.9 Cytoplasmic Donnan effectors

At steady state, as the resting membrane potential comes to a rest V_{rest} due to the permeabilities of potassium and sodium, the anion concentrations can be determined. If the movement of chloride ions is passive, then the Nernst equation for chloride is equal to the membrane potential at anterior and posterior $E_{Cl} = V_a = V_p = V_{rest}$.

$$[Cl^-]_i = [Cl^-]_e \frac{FV_{rest}}{RT} \quad (3.33)$$

At steady state, the course of neutrality and osmotic balance have been accomplished. For the anions to meet neutrality:

$$[Na^+]_i + [K^+]_i - [Cl^-]_i - [An^-]_i = -\Delta c \quad (3.34)$$

Where Δc is the small surplus of anions associated with the resting membrane potential V_{rest} .

$$\Delta c = -\frac{V_{rest}C_m}{FV_{ol_{cell}}} \quad (3.35)$$

To meet the requirements of osmotic equilibrium condition:

$$[Na^+]_i + [K^+]_i + [Cl^-]_i + [An^-]_i = [Sol]_i = [Sol]_e \quad (3.36)$$

Where $[An^-]_i$ is given as:

$$[An^-]_i = \frac{[Sol]_i + \Delta conc}{2} - [Cl^-]_i \quad (3.37)$$

3.10 Steady state

In a steady state, the model of the two-cell compartment acts like a singular cell. The external, cytoplasmic, and transmembrane currents on the anterior and posterior are equal based on **Figure 3.1**. [1] Therefore, approximating the equation (3.6) to have an endogenous electric field of zero proves that the steady state of a two-compartment cell connected via gap-junction does not produce any significant electric field if both cells experience the same intake and outtake.

Parameter	Unit	Anterior	Posterior
C_m	pF	20	20
R	$J/mol \cdot K$	8.314	8.314
T	K	310	310
F	C/mol	96.485	96.485
A	m^2	1×10^{-5}	1×10^{-5}
L	m	1×10^{-10}	1×10^{-10}
$D_{\text{permeant ions}}$	m^2/s	9×10^{-11}	9×10^{-11}
$D_{\text{impermeant ions}}$	m^2/s	9×10^{-14}	9×10^{-14}
P_{Na}	$\mu m^3/s$	1.51	1.51
P_K	$\mu m^3/s$	20	20
P_{Cl}	$\mu m^3/s$	2.5	2.5
P_{H_2O}	$\mu m^3/s$	2	2
$P_{Na} : P_K : P_{Cl}$	-	0.0075:1:0.125	0.0075:1:0.125
Vol_{cell}	μm^3	2000	2000
V_{rest}	mV	-70.22	-70.22
$[Na^+]$	mM	152/7.84	152/7.84
$[K^+]$	mM	3/147.16	3/147.16
$[Cl^-]$	mM	135/9.74	135/9.74
$[An^-]$	mM	20/145.26	20/145.26

The remainder of Scientific Methods will focus on maximizing the cytoplasmic potential voltage ΔV_{cyt} due to the relation of equation (2.1).

3.11 Maximizing endogenous electric field

This paper focuses on obtaining the most optimal endogenous electric field. We can achieve this from equation (2.1) by finding the endogenous voltage potential. Firstly, by observing the ratio of P_{Na+} and P_{K+} , we can determine that the higher the ratio, the higher the electric potential. Since we are limited to 2, 1, and $\frac{1}{2}$ the permeability multipliers, we set the P_{Na+} to twice the permeability while setting the potassium permeability P_{K+} to half the permeability. Implying that there will be more of an inflow of sodium and half the outflow of potassium, causing more membrane potential to increase since there is a surplus of cations. The ATPase pumps will work during this time due to ion homeostasis sensory. At this point, ions and anions will move across the cytoplasm from the anterior to the posterior, causing drift and diffusive currents. That being said, it is essential to mention that during the $4\times$ ratio uptake of ions, the posterior cell goes through regular steady-state conditions mentioned in Table 1 in the first chapter. Therefore, the movement from anterior anions and cations generates currents into endogenous voltage potential. The current on the anterior side would be negative due to the movement of ions and cations towards the posterior side, causing a positive current into the posterior side, thus generating voltage potential through equation 3.6.

Maximizing the electric field more, it is essential to note that the axial or cytoplasmic resistance affects the voltage potential, as seen in equation (3.9). Therefore, the resistance relationship in equation (3.11) shows us that increasing the Δx would increase the resistance, and we mentioned that the variable represents the elongation of the gap junction. According to the relation, elongating the gap junction increases the resistance and the cytoplasmic voltage potential.

To summarize, we theoretically determined that by increasing the ratio between sodium and potassium permeability leak and elongating the size of the gap junction Δx , we would obtain a high endogenous electric field. However, it is critical to note that there are limitations in this simulation. Otherwise, we can elongate the gap junction to infinity, continuously increasing the voltage potential. In the following chapter, parameters will be introduced to stay within the realms of reality.

4 Results

4.1 Parameters

Allowing the ions to leak at a higher/slower rate into/out of the cell causes a surplus of ions, which can cause a higher voltage within the cell. The objective is to set different parameters to maximize the endogenous electric field. In the previous section, we've observed some theoretical values that can optimize the voltage potential. By doing so, we are proportionally increasing the electric field since the diameter of the cell remains constant throughout this simulation with $10\mu\text{m}$.

The size of the gap-junction, according to (3.10), increases the resistance and the voltage. In theory, increasing the size of the gap-junction can lead to infinitely growing resistance, and to stay within the constraints of reality, setting an observational limit to the resistance seems appropriate. According to a simulation study done by Alexandra P. Henriquez on the "Influence of Dynamic Gap Junction Resistance on Impulse Propagation in Ventricular Myocardium," the limit to the resistance was set to $160.51\text{ M}\Omega$.^[5]

Another parameter to look out for is the ion movement through leaks. The two significant ions to look out for are the permeability of sodium Na^+ and potassium K^+ . Observation and calculation show that having a surplus of Na^+ and K^+ provides a more significant current inside the cell through diffusion and drift. Through careful consideration, we set the leak channels on the anterior side of the cell to flow twice the concentration of sodium ions into the cell while only leaking half the potassium amount inside the cell towards the outside, causing a surplus of ions and an increase of membrane potential.

Lastly, to maximize the largest endogenous electric field, we must observe the limitations observed through different scientific literature. A scientific book written by Richard Nuccitelli, "Current Topics in Developmental Biology," goes into endogenous electric fields in wound healing. This chapter in the book focuses on the epithelial wound generating an electric field that has been measured to be $40\text{-}200\text{ mV/mm}$.^[3]

The results in the next section will aim to find our results within these limitations of the electric field by modifying the parameters set above. The simulation aims to set different concentrations and loop over the gap junction's size.

4.2 Data Analysis

From the scientific methods covered in this paper, two factors influence the endogenous electric field: 1- the increased ratio of permeability from one cell and 2- the cell elongation. The important note is that there needs to be an initial noteworthy cytoplasmic voltage to keep increasing it via elongation of the gap junction. At the steady state of both cells, elongating the cell wouldn't increase the cytoplasmic voltage since there isn't a significant one to begin with. Therefore, manipulating the anterior permeability of ions is needed to create an initial membrane voltage. The posterior cell goes through standard steady-state values covered in the table of section 3.10. Once ions have circulated into the cell, ions move toward the posterior cell through the gap junction. The movement of ions creates the diffusive and drift current, which is calculated as the cytoplasmic current. The larger the current is the more prominent the cytoplasmic voltage becomes due to Ohm's law. Elongating the gap junction between the posterior and anterior cells improves the resistance of the gap junction. The gain of resistance improves the cytoplasmic voltage. Following Ohm's law, $V=IR$, if there is no current, there is no electric potential because there will always be resistivity between cells. Therefore, it is important to have some differences in permeability between cells to achieve some cytoplasmic current.

4.2.1 Anterior double P_{Na} and half P_K

The PA-CD model breaks symmetry by requiring the compartmentalized cell to change the permeability leak of sodium or potassium on the anterior or posterior side of the cell. As opposed to increasing both ends, this would achieve no endogenous electric field. Thus, a change in permeability would result in a change in diffusion and drift.

In the simulation, we set the permeability of sodium to be twice the amount and reduced the permeability of potassium by half in the anterior cell. In doing so, the ratio of permeability between sodium in potassium ends up at 0.302. From the background and context chapter, Zero Dimension Steady State, the ratio increases the transmembrane potential, in our case, V_a . Using equation (3.27), the result is -55 millivolts for the anterior voltage mirrored by the posterior membrane potential. Moreover, the exterior voltage produces the ohmic relation of exterior current and resistance, where the exterior current is the transmembrane current for each ion represented in equation (3.19), and the exterior resistor is given by one megaohm. Calculating the exterior voltage to be 0.04 millivolts.

From the exterior, anterior, and posterior voltages, the cytoplasmic voltage is calculated with Kirchoff's law, equation (3.6), to be 0.04 millivolts. By changing the permeability ratio, we obtained a positive, slightly significant cytoplasmic voltage of 0.4 millivolts per millimetre by keeping the gap junction at 10 microns.

Table 4.1 **Before and After steady state**

Parameters	Before	After
V_a	-70.2 mV	-55.4 mV
V_p	-70.2 mV	-55.4 mV
V_{ext}	0.083 mV	0.0433 mV
V_{cyt}	-0.083 mV	0.0429 mV
E_{cyt}	-0.83 mV/mm	0.429 mV/mm

Modifying the permeability gave us a positive cytoplasmic voltage potential, which gave us a positive endogenous electric field. Let us now focus on elongating the gap junction.

4.2.2 Elongation of gap junction

From the previous subsection, we are continuing with the permeability ratio at 0.302 by keeping the permeability of sodium leakage twice and half the permeability of potassium leakage. That way, we create some symmetry breaking. Additionally, by elongating the cell, the drift and diffusive currents going through the gap junction will experience more resistance. The effective diffusion D_{eff} is the variable to look out for as it contains the diffusion D constant, the reference size of the cell Δx_{ref} , and the gap junction separation Δx .

In the simulation, the diffusion and reference size of the cell are set, and the effective diffusion is a function of Δx , which is the elongation process. We loop over our simulation and continuously increase the effective diffusion, increasing cytoplasmic voltage, as shown in Figure 4.1. Showing an inverse-like function, we show that the denominator rises near zero, giving us a cytoplasmic voltage of 7.47 millivolts at Δx around 2.56 millimetres.

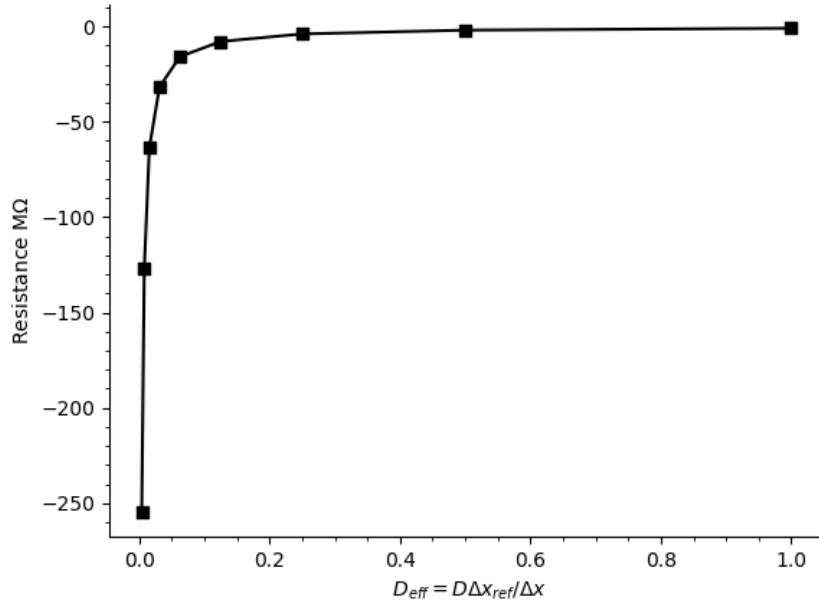


Figure 4.2 **Gap junction resistance as effective diffusion.** The effective diffusion works as a function of Δx_{ref} , Δx , and diffusion D , increases when Δx is at higher values and decreases at lower values. The elongation of the cell describes a negative asymptotic relation with high values reaching near $-250 \text{ M}\Omega$ and near $0 \text{ M}\Omega$ at values equal to Δx_{ref} .

We verify the resistance increase by elongating the cell within the effective diffusion function. We know that the relation inside the cytoplasm results in an Ohmic relationship. Therefore, knowing the cytoplasmic currents, through the diffusion and drift of ions and anions, and the cytoplasmic voltage, we check to see the relation of increasing the Δx and the resistance of the gap junction, the cytoplasmic voltage, and the field strength of the endogenous electric field, from Figure 4.2 and 4.3, we see that elongating the cell produces higher resistance and higher cytoplasmic voltage if we look at the left-most area of both graphs, which is an indication that the effective diffusion is minimal and the relations grow because of it.

Table 4.2 Results from $2P_{Na}$, $0.5P_K$, and decrease of D_{eff}

D_{eff}	1	0.5	0.25	0.125	0.0625	0.03125	0.0156	0.00781	0.0039
$R_{cyt}(M\Omega)$	-0.99	-1.99	-3.97	-7.94	-15.88	-31.75	-63.52	-127.17	-255
$V_{cyt}(mV)$	0.043	0.086	0.17	0.34	0.66	1.26	2.37	4.33	7.47
$I_{cyt}(pA)$	-43.23	-43.08	-42.79	-42.25	-41.29	-39.73	-37.38	-34.02	-29.3
$E_{cyt}(mV/mm)$	0.43	0.86	1.7	3.35	6.56	12.62	23.75	43.26	74.73

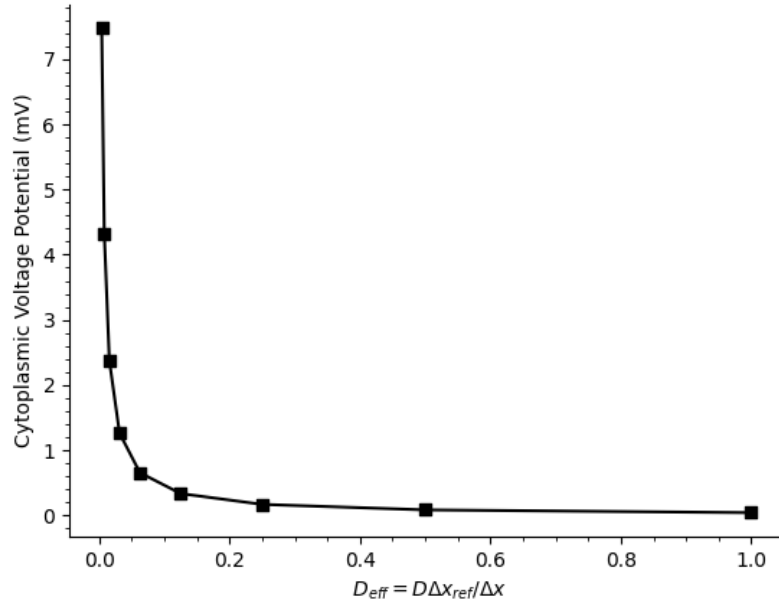


Figure 4.2 **Cytoplasmic voltage per effective diffusion.** The cytoplasmic voltage potential as the effective diffusion. The graph resembles an asymptotic function, as Δx increases the resulting cytoplasmic voltage increases. Contrarily, as the elongation of the cell Δx resembles the reference size of the cell Δx_{ref} the voltage is closer to zero.

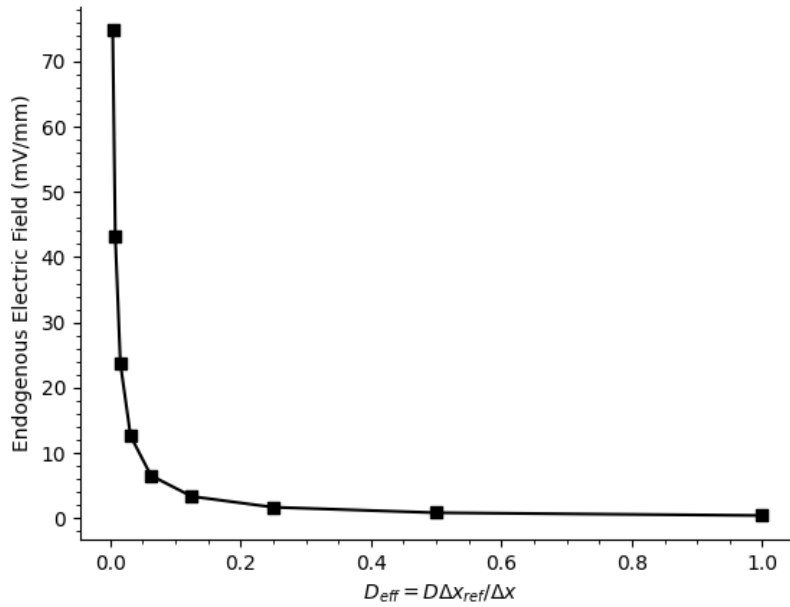


Figure 4.3 **Endogenous electric field per effective diffusion.** Endogenous electric field as a function of effective diffusion. The graph resembles an asymptotic function, as Δx increases the resulting endogenous electric field increases. Contrarily, as the elongation of the cell Δx resembles the reference size of the cell Δx_{ref} the electric field is closer to zero.

The anterior side of the cell goes through changes in leak permeability, which results in membrane potential, which we are able to use to calculate the cytoplasmic voltage. The cytoplasmic voltage is then being used to measure the endogenous electric field. Notably, this electric field depends on separating the two compartmentalized cells. By keeping the permeabilities constant and increasing the gap junction size between the two cells, we are increasing the resistance as per equation (3.11). While the resistance progressively increases, the cytoplasmic voltage increases, causing more electric fields.

Following our limitations, the maximal separation that can only be obtained is 2.56 mm, equivalent to $\approx 255 \text{ M}\Omega$ in resistance for the gap junction.

Table 4.3 provides the information of the different combinations of multiplication factor of the leak permeability for each ion and the resulting endogenous electric field from the maximized gap-junction distance and resistance.

Table 4.3 **Endogenous Electric Field based on change in leak permeable parameters.**

Leak Permeability	Endogenous Electric Field (mV/mm)								
	$\Delta x = 10\mu m$	$20\mu m$	$40\mu m$	$80\mu m$	$160\mu m$	$320\mu m$	$640\mu m$	$1280\mu m$	$2560\mu m$
$2P_{K^+} : 2P_{Na^+}$	0.1	0.2	0.4	0.79	1.55	3.0	5.65	10.5	18.44
$P_{K^+} : 2P_{Na^+}$	0.28	0.55	1.1	2.16	4.2	8.08	15.1	27.2	46
$0.5P_{K^+} : 2P_{Na^+}$	0.43	0.86	1.7	3.35	6.57	12.6	23.7	43.26	74.73
$2P_{K^+} : P_{Na^+}$	-0.15	-0.3	-0.6	-1.18	-2.35	-4.6	-8.88	-16.5	-29.05
$2P_{K^+} : 0.5P_{Na^+}$	-0.29	-0.58	-1.15	-2.26	-4.37	-8.33	-15.6	-28.5	-49.58
$P_{K^+} : P_{Na^+}$	$\approx \times 10^{-11}$								
$P_{K^+} : 0.5P_{Na^+}$	-0.16	-0.32	-0.63	-1.23	-2.34	-4.35	-7.96	-14.3	-24.99
$0.5P_{K^+} : P_{Na^+}$	0.13	0.26	0.51	1.03	2.04	4.03	7.86	14.9	27.05
$0.5P_{K^+} : 0.5P_{Na^+}$	-0.05	-0.1	-0.18	-0.33	-0.55	-0.83	-1.15	-1.48	-1.84

Based on the data, at $255 \text{ M}\Omega$ for the resistance, the highest electric field obtained is 74.73 mV/mm , falling within the experimental range observed by R. Nuccitelli. Another notable consideration is -49.58 mV/mm , which would mean that the electric field would be relatively positive from the posterior side of the cell travelling in the opposite direction compared to the previous value observed.

4.2.3 Anterior Posterior symmetry breaking

The last section discussed different combinations to maximize the endogenous electric field. These combinations involved changing the permeability of the sodium and potassium gated channel on the anterior side of the cell. Some observations to add are breaking symmetry by changing both the anterior and posterior leak permeability.

We create larger endogenous electric fields by breaking symmetry and involving different leak permeabilities for the anterior and posterior. From what we see in the last subsection, doubling P_{Na+} and halving P_{K+} on the anterior cell depolarize the membrane. However, by halving the P_{Na+} and doubling P_{K+} , we are hyperpolarizing the posterior cell, resulting in a significant movement of diffusion and drift in the cytoplasm, resulting in large currents and voltage potential.

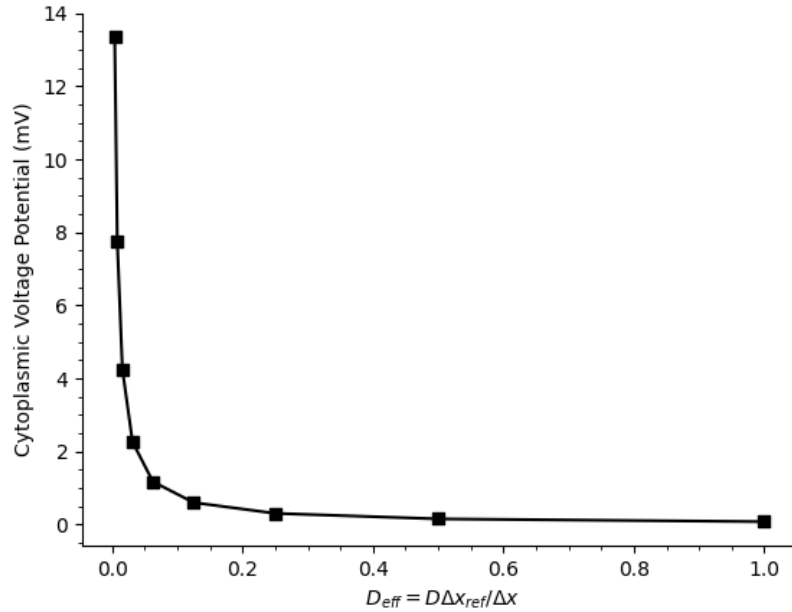


Figure 4.4 **Cytoplasmic voltage per effective diffusion.** Endogenous electric field as a function of effective diffusion. The graph resembles an asymptotic function, as Δx increases the resulting endogenous electric field increases. Contrarily, as the elongation of the cell Δx resembles the reference size of the cell Δx_{ref} the electric field is closer to zero (0.429 as per table 4.1).

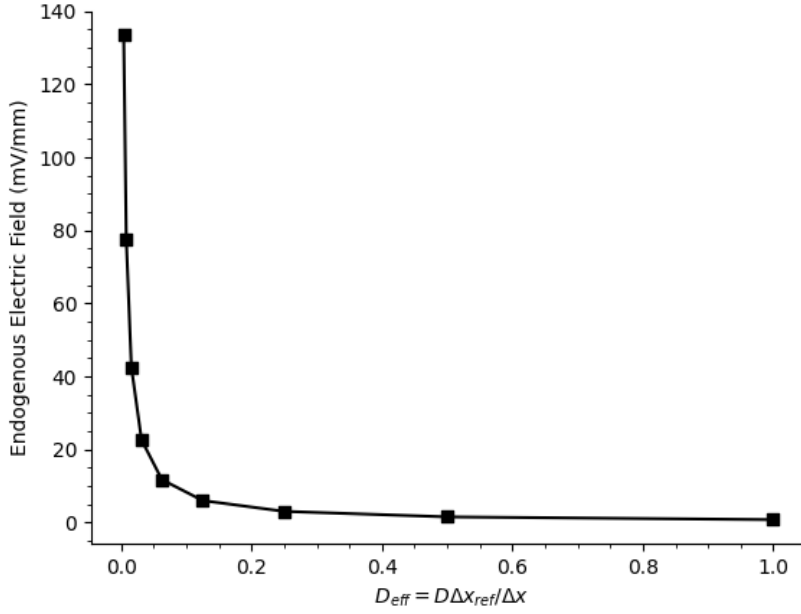


Figure 4.5 **Endogenous electric field per effective diffusion**. Endogenous electric field as a function of effective diffusion. The graph resembles an asymptotic function, as Δx increases the resulting endogenous electric field increases. Contrarily, as the elongation of the cell Δx resembles the reference size of the cell Δx_{ref} the electric field is closer to zero (0.429 as per table 4.1).

While keeping the same constraints for the gap junction resistance and maintaining the smallest effective diffusion. The result obtained for the endogenous electric field is 133.43 millivolts per millimetre by reducing posterior and increasing anterior sodium leak and increasing posterior and reducing anterior potassium leak. Following Figure 2.3, in the Background and Context chapter, we increase the ratio to 16 times the ratio of anterior and posterior permeability. However, looking at the cytoplasmic voltage, it achieves close to 14 millivolts at small effective diffusion but achieves 0.76 millivolts per millimetre at the reference length Δx_{ref} from the result of 0.076 millivolts of cytoplasmic voltage. Therefore, by elongating the cell and reducing the effective diffusion, we nearly 175x the endogenous electric field while staying within the constraints.

Table 4.4 **Endogenous Electric Field based Anterior Posterior Permeability Ratios**

Ant/Post Ratios	Endogenous Electric Field (mV/mm)								
	$\Delta x = 10\mu m$	$20\mu m$	$40\mu m$	$80\mu m$	$160\mu m$	$320\mu m$	$640\mu m$	$1280\mu m$	$2560\mu m$
$(P_{Na} : P_K)_a : (P_{Na} : P_K)_p$	$\approx \times 10^{-11}$								
$4(P_{Na} : P_K)_a : \frac{1}{4}(P_{Na} : P_K)_p$	0.77	1.53	3.04	6.00	11.72	22.57	42.58	77.62	133.43
$(2P_{Na} : \frac{1}{2}P_K)_a : (\frac{1}{2}P_{Na} : P_K)_p$	0.56	1.11	2.20	4.32	8.37	15.98	29.93	54.57	94.88
$(2P_{Na} : \frac{1}{2}P_K)_a : (P_{Na} : 2P_K)_p$	0.64	1.29	2.56	5.08	10.01	19.45	36.92	67.43	115.54
$\frac{1}{4}(P_{Na} : P_K)_a : 4(P_{Na} : P_K)_p$	-0.77	-1.53	-3.04	-6.00	-11.72	-22.57	-42.58	-77.62	-133.43

4.3 Discussion

The PA-CD model, a two-compartment cell connected by a gap junction, went through a series of tests in breaking symmetry, where the permeability ratios that we saw in Chapter 2 have been explored and analyzed for a better understanding of maximizing the endogenous electric field while the cell is polarized. Two methods that allowed us to break symmetry of the PA-CD model were to change the permeability ratios between the potassium and sodium ions while ignoring the effects of the chloride ions, and to decrease the effective diffusion by elongating the gap junction of the cells resulting in a more significant resistance.

While simulating the trials and increasing the gap junction, we kept in mind the limitations of other scientific papers such as Richard Nuccitelli's "Current Topics in Developmental Biology," where the author focuses on epithelial wound generating 40 to 200 millivolts per millimetre endogenous electric fields, and Alexandra P. Henriquez, "Influence of Dynamic Gap Junction Resistance on Impulse Propagation in Ventricular Myocardium," where the author simulated up to a resistance of 160 megaohms. From the results obtained and modifying the resistance threshold at 255 megaohms, we've received the highest simulated endogenous electric fields at 133.43 millivolts per millimetre when both anterior and posterior cells experienced different permeability ratios, where the collective ratio was $16 P_{ant} : P_{post}$. Meanwhile, maintaining the posterior cell to standard steady-state parameters and fluctuating the ratio of the anterior permeability, the highest endogenous electric field attained was 74.73 millivolts per millimetre at the highest distance, the gap junction distance achievable.

5 Conclusion

This study delved into the intricate mechanisms that govern excitable cells' ion flux and polarization in a posterior-anterior cell connected by a gap junction. By investigating the charge difference model, we explored the symmetry breaking through cell elongation and the ion permeability ratio influencing the endogenous electric field.

The investigation began with an overview of electric fields in wound healing. A paper by Paulo Luiz et al. discusses the fluctuation of electric fields in wound healing, which sets the foundation for understanding the background of endogenous electric fields. Then, an overview of the role of ion homeostasis is provided in maintaining cellular equilibrium through passive and active ion movements, highlighting the significance of polarization through the permeability ratio of potassium and sodium.

Through theoretical analyses, we investigated the circuitry of a two-compartment cell and derived expressions for currents, voltages, and resistance that contribute to the cells' steady state. We aimed to optimize the endogenous electric field within realistic constraints. By adjusting parameters such as the elongation of the cell and the permeability ratios, we sought to maximize the cytoplasmic voltage and consequently enhance the endogenous electric field.

Symmetry breaking was an excellent strategy for disrupting equilibrium in the posterior-anterior charge difference model, where altering permeability ratios between anterior and posterior and elongating the gap junction contributed to higher cytoplasmic voltage and electric field strength. Our findings demonstrate that by manipulating the combination of ion permeability and gap junction characteristics, we achieved significant adjustments in endogenous electric fields compared to a symmetric coupled cell. Moreover, the results align themselves with the limitations of experimental work.

Our study opens avenues for further research into understanding the complexity of endogenous electric fields in biological cells. We gain a deeper understanding of the physiology and the potential strategies in wound healing and tissue regeneration.

References

- [1] Ziyi Liu, Developing Tools towards Ion Homeostasis in Spatially Polarized Excitable Cells. Department of Physics, Faculty of Science, University of Ottawa.
- [2] Schatten, Gerald. Current Topics in Developmental Biology. Elsevier/Academic Press, 2005.
- [3] Farber, Paulo Luiz, et al. “Electric Factors in Wound Healing.” Advances in Wound Care, U.S. National Library of Medicine, Aug. 2021, www.ncbi.nlm.nih.gov/pmc/articles/PMC8236302/#:~:text=The%20movements%20of%20ions%20create,endogenous%20electric%20field%20is%20created.&text=Electric%20fields%2C%20both%20endogenous%20and,migration%20and%20modulate%20wound%20healing.
- [4] Dijkstra, K., J. Hofmeijer, S.A. van Gils, and M.J.A.M. van Putten. 2016. A Biophysical Model for Cytotoxic Cell Swelling. J. Neurosci. 36:11881–11890. doi:10.1523/JNEUROSCI.1934-16.2016.
- [5] Influence of Dynamic Gap Junction Resistance on Impulse Propagation in Ventricular Myocardium: A Computer Simulation Study: Biophysical Journal, [www.cell.com/fulltext/S0006-3495\(01\)75859-6](http://www.cell.com/fulltext/S0006-3495(01)75859-6). Accessed 22 Apr. 2024.
- [6] Morris, Catherine E., et al. “The Donnan-Dominated Resting State of Skeletal Muscle Fibers Contributes to Resilience and Longevity in Dystrophic Fibers.” Journal of General Physiology, The Rockefeller University Press, 3 Jan. 2022, rupress.org/jgp/article/154/1/e202112914/212743/The-Donnan-dominated-resting-state-of-skeletal.